STScI | SPACE TELESCOPE SCIENCE INSTITUTE

Instrument Science Report COS 2017-06(v2)

Spectral Resolution of COS/FUV at Lifetime Position 3

Julia Roman-Duval[1], Cristina Oliveira[1], Paule Sonnentrucker[1]

[1] Space Telescope Science Institute, Baltimore, MD

December 12, 2017

ABSTRACT

In order to overcome gain-sag effects, the position of spectra on the COS FUV detector was moved from lifetime position 2 (LP2), located +3.5" above the original lifetime position (LP1), to lifetime position 3 (LP3), at −2.5" below LP1, on February 9, 2015. Special calibration programs were undertaken to characterize the detector at the LP3 location. In this ISR, we characterize the spatial and spectral resolution at the third COS FUV lifetime position. Code V Optical models of the COS line spread functions (LSFs) are generated for modes of the M and L gratings, accounting for mid-frequency wavefront errors (MFWFE). In order to validate the modeling of the COS FUV LSFs, we perform a comparison of spectral line profiles between, on the one hand, COS FUV spectra of SMC O star AV75 acquired at the third lifetime position, and on the other hand previous STIS E140M spectra convolved with models of the COS FUV LSFs at LP3. Our analysis shows that the model LSFs are consistent with the observations within the measurement errors.

Contents

1. Introduction

A limited amount of charge can be extracted from the FUV cross-delay lines of the COS FUV detector. As a result, the gain in a pixel — the number of electrons generated by an incident photon — decreases as the cumulative number of photons ever collected in that pixel increases. This effect, known as "gain-sag", leads to a localized loss of sensitivity with time. When the modal gain — defined as the peak of the gain distribution — becomes lower than about 2, the flux in that pixel cannot be recovered.

On July 23rd, 2012, the default location of COS FUV spectra was shifted from LP1 to LP2, at 3.5" above LP1 in the cross-dispersion direction, and at -0.05" along the dispersion direction relative to the original lifetime position. FUV spectra were obtained at LP2 for about 2.5 years. In February 2015, science spectra were once again moved to a pristine region of the detector, from LP2 to LP3, located at -2.5" below LP1 (COS ISR 2016-01). Several special calibration programs were executed to calibrate the spectral resolution at LP3 (13931, "Third COS FUV Lifetime Position: Wavelength and Resolution Calibration (LCAL2)" PI Roman-Duval), the flux, flat-field, and spectral profiles (13932, "Third COS FUV Lifetime Position: Cross-Dispersion Profiles, Flux, and Flat-Field Calibration (LCAL3)", PI Debes), and the bright object aperture (BOA) performance (13933, "Third COS FUV Lifetime Calibration Program: Verification of FUV BOA Operations (LCAL4)", PI Fox).

Because the lifetime move involves a change in the optical path of FUV photons, changes in spectral and spatial resolution are expected. Thus, the resolution of the COS FUV modes at the third lifetime position needs to be calibrated. The COS Line Spread Functions (LSFs) are known to be non-gaussian due to mid-frequency wavefront errors (MFWFE), which are polishing errors on the primary and secondary HST mirrors (COS ISR 2009-01). Because the wings of the COS LSFs contain a significant fraction of the total power, a proper characterization of the COS LSFs is necessary to perform accurate line profile fitting, and to determine the feasibility and required exposure time of weak and/or narrow spectral features. While the contributions from MFWFE have remained the same with the COS FUV lifetime move, the LSFs resulting from the COS+OTA (optical telescope assembly) combination have changed.

We have modeled the COS FUV LSFs at LP3 using a code V optical model, and validated the model using observations with the COS FUV gratings at lifetime position 3. The observations for the medium resolution gratings were taken as part of Cycle 22 special calibration program 13931 ("Third COS FUV Lifetime Position: Wavelength and Resolution Calibration", PI: Roman-Duval), which obtained high S/N observations of the reddened SMC star AzV 75 for the purpose of characterizing the spectral resolution of G130M and G160M at LP3. For the G140L grating, the observations were taken as part of program 13635 ("FUV Focus Sweep Enabling Program for COS at LP3 (LENA2)"), which obtained G140L/1105 spectra of AzV 75 at different focii to determine the focus maximizing spectral resolution. The exposure at best focus was used in this analysis.

In this ISR, we describe the complete analysis of the COS FUV spectral resolution

at LP3 for all three FUV gratings (G130M, G160M, G140L).

2. Code V model of the COS/FUV LSFs at LP3

The Line Spread Functions (LSF) of all COS FUV settings at LP3 were modeled using code V, based on a model of the COS system provided by Tom Delker (Ball Aerospace) and updated by Erin Elliott (see COS ISR 2013-07). The move to the second lifetime position incurred a change in field angle. Hence, pointing was adjusted to -2.5 arcsec in the $+$YUSER direction in COS coordinates. This was done by adding a $-$ 2.5 arcsec shift in the cross-dispersion direction to the original design field point, given by $\mathrm{X}_{CodeV} = \mathrm{X}_{user} = -0.000725°$, $\mathrm{Y}_{CodeV} = \mathrm{Y}_{user} = 0.089939°$.

The LP3 grating locations (rotation and focus) were set to be equal to those of LP2 (see COS ISR 2013-07). This is a valid estimate of the grating locations because the LP3 field point (-2.5 arcsec) is almost opposite the LP2 field point ($+3.5$ arcsec). The aberrations in the system are primarily astigmatism and astigmatism has an odd dependence on field; therefore, opposite field points will have astigmatism that is opposite in sign but similar in magnitude (see also Report_COSModelsAndData_Elliott_2014_06_05_v09.pdf, LSFEstimatesForCOS_Elliott_v22.pdf and GratingLocations_v08.xlsx).

The raw Code V PSFs, sampled every 1Å, were imported into Mathematica and converted to 6×6 μm pixels. Detector blur was then added by convolving the PSF array with a Gaussian kernel with σ_x = 2 pixels (12 μm) in the dispersion direction and σ_y = 1 pixel (24 μm) in the cross-dispersion direction. All PSF arrays were then normalized so that they contained the same total intensity. Finally, the arrays were summed along the cross-dispersion direction to generate the final Line Spread Function. The arrays were summed along the dispersion direction to generate the final Cross-Dispersion Spread Functions (CDSF). All LSFs and CDSFs were normalized to have a maximum height of 1. The LP3 LSFs and CDSFs are available at
`http://www.stsci.edu/hst/cos/performance/spectral_resolution/`.
The LP3 LSF for the G130M/1309 cenwave at 1302 $\AA$ is compared to the LP1 and LP2 LSF of the same setting in Figure 1. The modeled spectral resolution at LP1 is significantly better than at LP2 and LP3, but remains roughly identical between LP2 and LP3. This behavior is shown as a function of wavelength in Figure 2.

3. Validation of the model LSFs using COS FUV observations

3.1 Data

We designed a special calibration program (PID 13931, "Third COS FUV Lifetime Position: Wavelength and Resolution Calibration (LCAL2)", PI Roman-Duval) to validate the Code V models of the COS/FUV LP3 LSFs with on-orbit observations. We followed the same approach as for the validation of the COS/FUV model LSFs at LP2. We first obtained high S/N data (S/N = 60 per resolution element) of SMC star AzV 75, a reddened O5 III star in the SMC (E(B-V) = 0.16) previously observed with STIS/E140M.

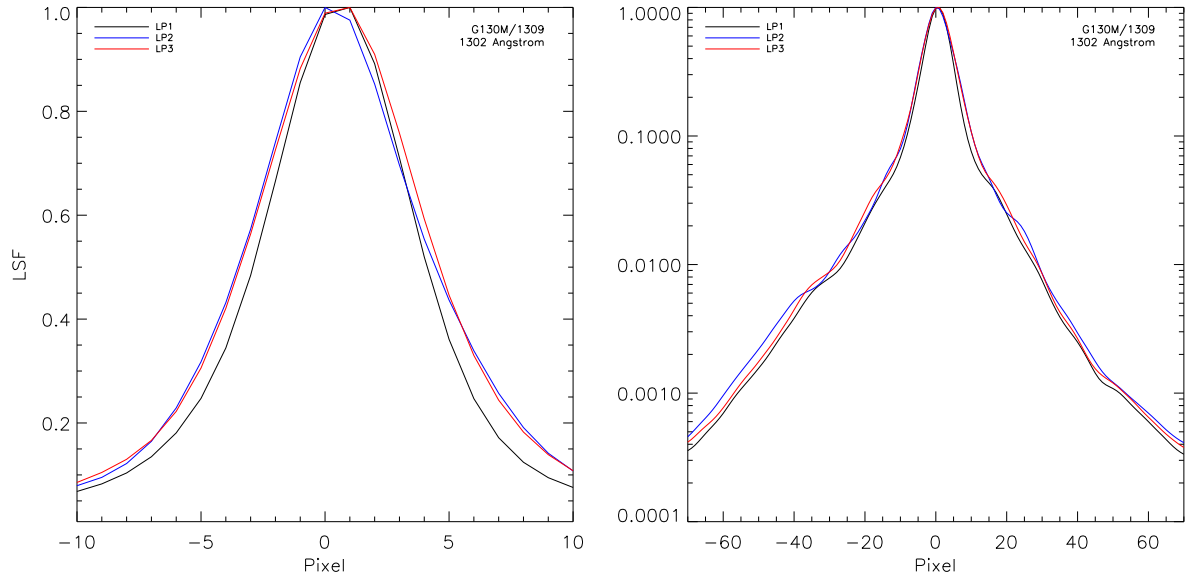

Figure 1.: Comparison of the LP1 (black), LP2 (blue), and LP3 (red) COS/FUV LSF for the G130M/1309 setting at 1302 Å. The left panel shows a zoom on the core of the LSF in linear y-scale, while the right panel includes the non-gaussian wings of the LSF, in logarithmic y-scale

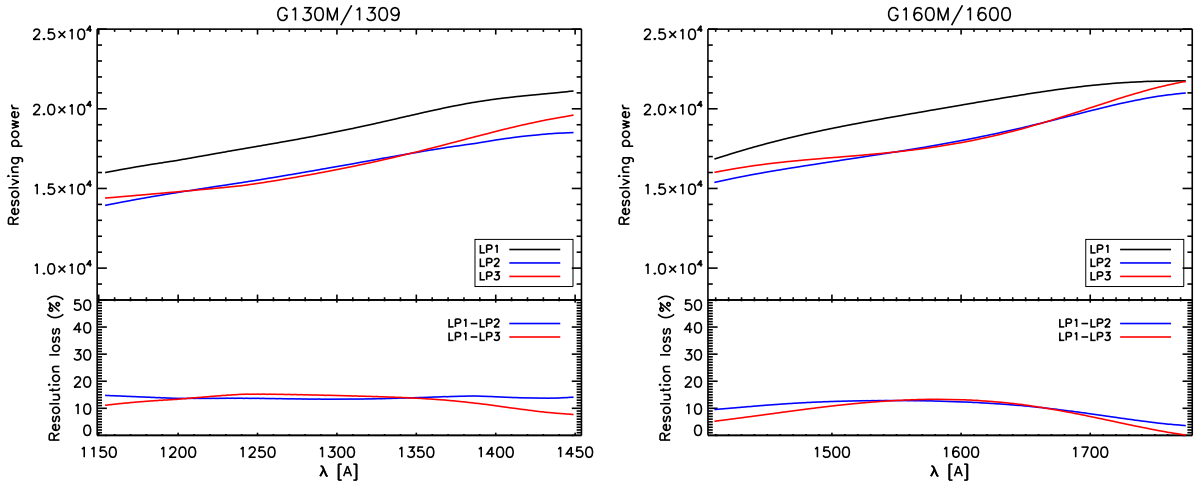

Figure 2.: (Top) Comparison of the LP1 (black), LP2 (blue), and LP3 (red) COS/FUV resolving power for the G130M/1309 (left) and G160M/1600 (right) settings, as a function of wavelength. The resolving power is computed as the ratio of the LSF FWHM and wavelength. (Bottom) Fractional resolution loss incurred by the move from LP1 to LP2 (blue) and LP1 to LP3 (red).

This target was also used for measuring the spectral resolution at LP2, and serves as our wavelength calibration monitoring target. AzV 75 was chosen because 1) it is in the appropriate brightness range for COS, not exceeding the local or global count rate, and yet allowing a high signal-to-noise to be reached relatively quickly; and 2) it is one of the most reddened stars observed with STIS/E140M, ensuring the presence of numerous ISM lines, unresolved and saturated.

Program 13931 obtained exposures with the G130M 1222 (2000s), 1291 (800s), 1327 (800s), G160M 1577 (1800s) and 1623 (1600s) settings. Extreme cenwaves were chosen to sample the entire range of wavelengths covered by each grating. Since the 1222 cenwave has an extreme focus, determined to optimize the spectral resolution in the middle of FUVB, this setting was observed as well. In each case, the total exposure time was split equally amongst 4 FP-POS to maximize the S/N of the combined spectra. The program was packed into 4 orbits and executed on July 13, 2015 (a first execution in March 2015 failed to guide star acquisition issues). Table 1 lists all the x1d exposures used in this analysis. In this analysis, we used the FP-POS combined x1dsum spectra.

The G140L observations of AzV 75 were acquired as part of enabling program LENA2 (13635, "FUV Focus Sweep Enabling Program for COS at LP3 (LENA2)", PI Hernandez), which aimed to determine the optimal focus of the G140L at LP3. The G140L observations consisted in 200s exposures at varying focii with the 1105 cenwave. The optimal focus was found to be at -673 motor steps (-138 from LP2), and corresponds to exposure lcil3aj3q, which is used for this analysis.

The STIS E140M spectra used in this analysis, with resolution R $\simeq$ 45,000 and covering the wavelength range 1100 Å — 1700 Å, were obtained as part of program 7437 (PI: Lennon), and retrieved from the MAST archive (exposures o4wr11010 and o4wr11020). STIS echelle spectra directly retrieved from the archive exhibit large spikes at regular intervals because orders are not combined. In order to mitigate this issue, we combined the echelle orders ourselves, and then co-added the two x1d spectra by weighing each exposure with the corresponding exposure times (2448 s and 3168 s respectively). The S/N of the combined spectrum varies between 10 and 20 per pixel across the wavelength range of the E140M at cenwave 1425. In the following analysis, we use this final co-added STIS spectrum.

3.2 Methodology

In order to validate the model LSF with on-orbit data, we compared line profiles (both unresolved, resolved, and saturated) observed in the LCAL2 spectra obtained at LP3 with line profiles in previous STIS high resolution echelle E140M spectra, convolved with the model COS FUV LSFs at LP3. The comparison of the STIS spectra convolved to COS resolution and the on-orbit COS unresolved and saturated complex line profiles allowed us to constrain the changes in the core and wings of the LSF respectively. First, the STIS spectrum was resampled on the same wavelength grid as the COS spectra. Second, the convolution was performed. The COS LSFs are sampled every 1 Å. The shape of the LSF varies with wavelength, as seen in the FWHM measured in the

Table 1. Exposures from 13931 (G130M and G160M) and 13635 (G140L) used in the characterization of the spectral resolution of the COS/FUV.

Grating	Cenwave	Exposure	FPPOS
G130M	1222	lcrs51dvq	1
		lcrs51dxq	2
		lcrs51dzq	3
		lcrs51e1q	4
	1291	lcrs51dlq	1
		lcrs51dnq	2
		lcrs51dpq	3
		lcrs51drq	4
	1327	lcrs51e5q	1
		llcrs51e7q	2
		lcrs51e9q	3
		lcrs51ebq	4
G160M	1577	llcrs51edq	1
		lcrs51efq	2
		lcrs51ejq	3
		lcrs51elq	4
	1623	lcrs51enq	1
		lcrs51epq	2
		lcrs51erq	3
		lcrs51etq	4
G140L	1105	lcil3aj3q	3

model LSFs (Figure 2). Hence, we split the resampled STIS spectrum in the corresponding number of wavelength intervals closest to each of the wavelength of the grid of COS LSFs, and applied the convolution to each interval using the appropriate LSF. The convolution algorithm used the IDL routine CONVOL with the NORMALIZE and EDGE_TRUNCATE keywords.

We identified numerous ISM lines in the AzV 75 spectra to compare line profiles in the STIS spectra convolved to COS resolution and in observed COS spectra at each of the extreme cenwaves of the G130M and G160M gratings, and the 1105 cenwave of the G140L grating. The observed COS spectra are affected by small shifts in wavelength between different cenwaves, due to residual effects of X-walk and an imperfect geometric distortion correction. Although these shifts, typically of magnitude $\pm$ 30 mÅ (or 3 pixels) for the M gratings, do not violate the accuracy requirements of the wavelength solution (see COS ISR 2013-06), they are large enough to appear very obvious when comparing spectra taken at different cenwaves. In each spectral window, we therefore cross-correlated the COS spectrum and the convolved STIS spectrum and aligned then before comparing them. We also cross-correlated the LP2 COS spectrum of AzV 75 taken as part of program 12805 (the LP2 equivalent of 13931) with the LP3 corresponding spectrum and aligned them for comparison as well, to estimate the resolution loss between LP2 and LP3.

Finally, we compared the synthetic ($f_s(\lambda)$) and observed ($f_o(\lambda)$) COS spectra in each spectral window, and computed the residual as $r(\lambda) = (f_o(\lambda) - f_s(\lambda))/f_s(\lambda)$.

While in principle the STIS echelle spectra should be de-convolved before applying the convolution with the COS LSFs, the large difference in spectral resolution between the STIS E140M grating (R $\simeq$ 45, 000) and the COS M gratings (R $\simeq$ 20,000), and even more so COS L grating (R $\simeq$ 2,500), is such that we can safely omit this difficult step. Indeed, the contribution from the STIS E140M FWHM would then only be at most 5% of the FWHM of the STIS E140M spectrum convolved with the COS M grating LSFs.

3.3 Results

The comparison between the STIS spectra convolved with the COS LSFs and the observed COS spectra are shown in Figures 3, 4, 5, 6,7, and 8 for the G130M/1222, G130M/1291, G130M/1327, G160M/1577, G160M/1623, and G140L/1105 settings, respectively. The black line corresponds to the COS LP2 spectrum, the blue lines show the convolved STIS spectra, and the red lines correspond to the observed COS LP3 spectra, binned by 5 pixels. Figures 3, 4, 5, 6, 7, and 8 also show the fractional residuals, which, in most cases, do not exceed 10%. There are some excursions to high fractional residual, but these are located in regions with very low counts, where the fractional residual is not well defined anyway. In the top left panel of Figure 3 corresponding to wavelength 1143 $\AA$, the STIS spectrum does not extend down to such short wavelength, and as a result, we only compare the LP2 and LP3 line profiles. Hence, we cannot com-

pute residuals with respect to the convolved STIS spectrum for this wavelength.

Narrow, unresolved lines constrain the core (or FWHM) of the LSF best. On the other hand, the non-gaussian wings of the COS LSFs are better revealed in complex or blended, saturated wide profiles. Figures 3, 4, 5, 6, 7, and 8 show that the model of the core and wings of the COS LSFs matches the observations very well: the fractional residual is within the error bars in all unresolved ISM lines. Note that the fractional residual in the bottom of saturated profiles, where the count rate is very low, is meaningless.

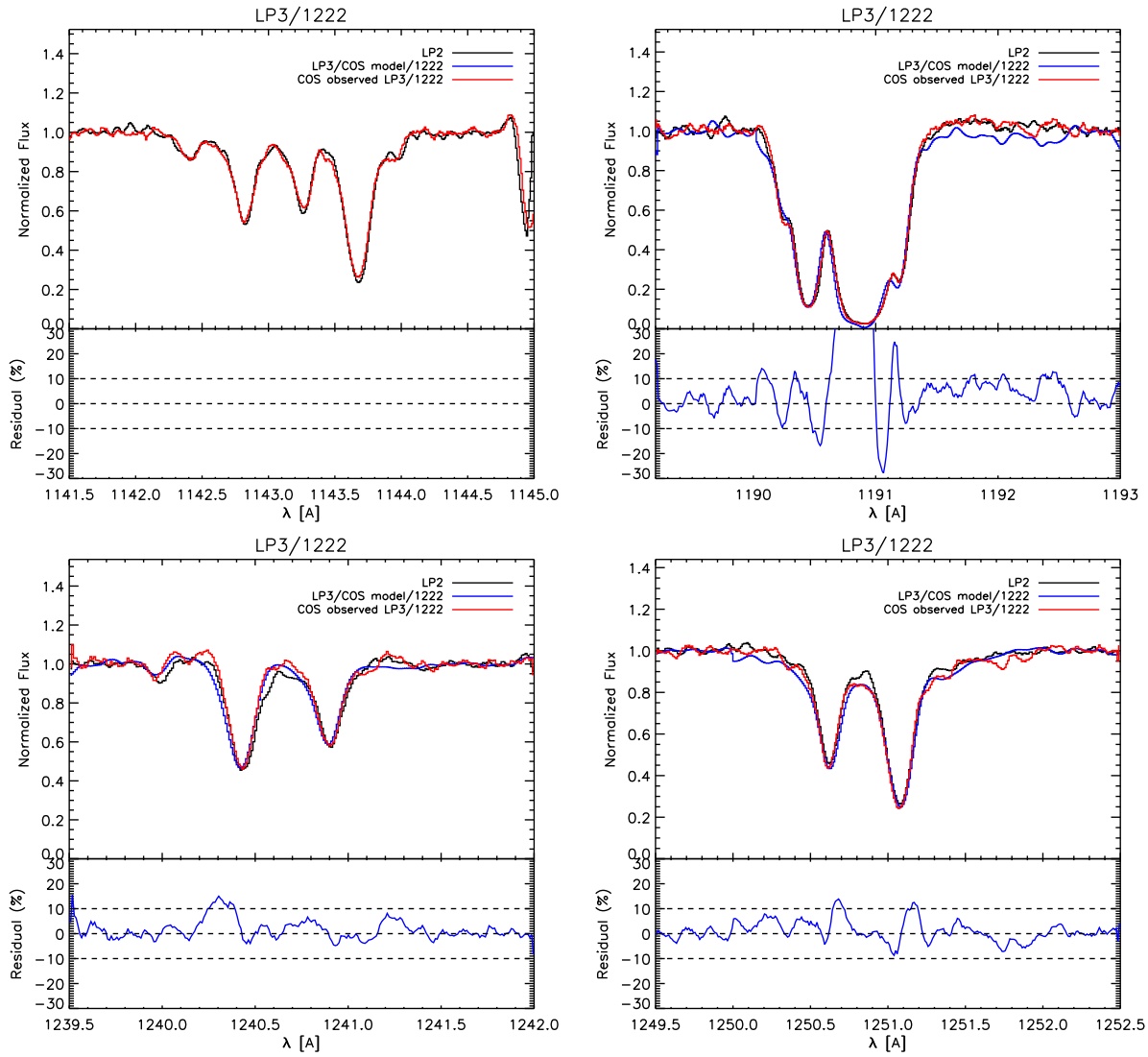

Figure 3.: Comparison between the line profiles obtained with the G130M 1222 at LP2 (black), LP3 (red), and the STIS E140M spectrum convolved with the LP3 COS model LSFs. The residuals shown in the bottom sub-panels correspond to the fractional difference between the observed COS spectra and the STIS spectrum convolved with the COS model LSFs at LP3 (i.e., between the blue and red lines). In the top left panel corresponding to wavelength 1143 $\mathring{A}$, the STIS spectrum does not extend down to such short wavelength, and as a result, we only compare the LP2 and LP3 line profiles. Hence, we cannot compute residuals with respect to the convolved STIS spectrum for this wavelength.

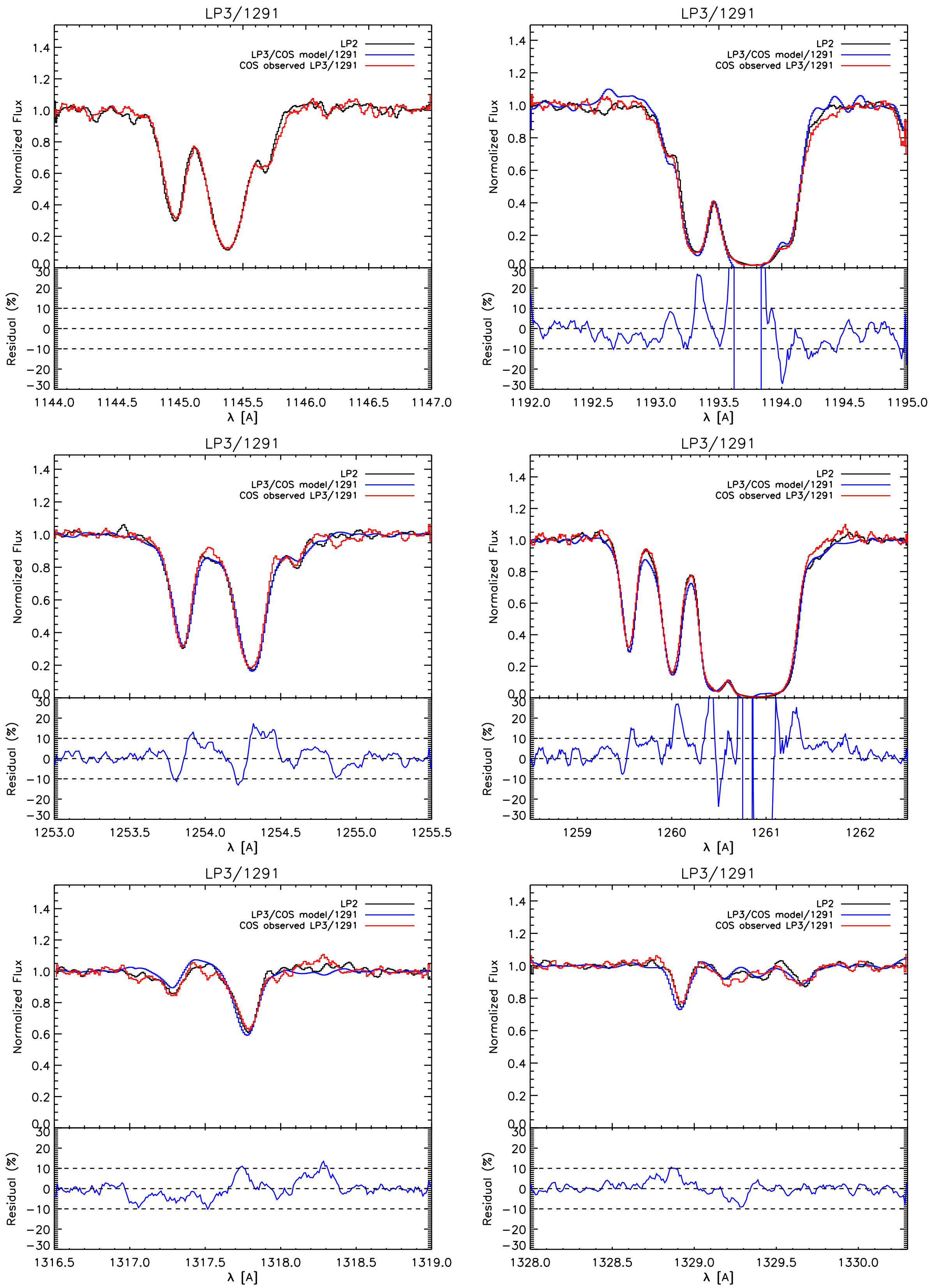
LP3/1291
LP2
LP3/COS model/1291
COS observed LP3/1291
Normalized Flux
Residual (%)
λ [A]
1144.0
1144.5
1145.0
1145.5
1146.0
1146.5
1147.0
1192.0
1192.5
1193.0
1193.5
1194.0
1194.5
1195.0
1253.0
1253.5
1254.0
1254.5
1255.0
1255.5
1259
1260
1261
1262
1316.5
1317.0
1317.5
1318.0
1318.5
1319.0
1328.0
1328.5
1329.0
1329.5
1330.0

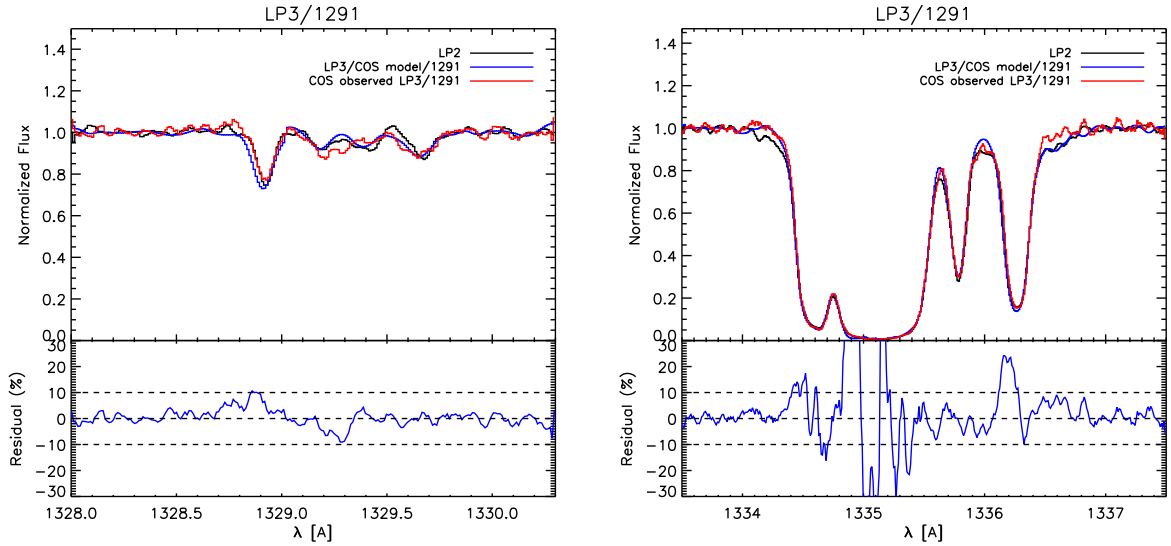

Figure 4.: Comparison between the line profiles obtained with the G130M 1291 at LP2 (black), LP3 (red), and the STIS E140M spectrum convolved with the LP3 COS model LSFs. The residuals shown in the bottom sub-panels correspond to the fractional difference between the observed COS spectra and the STIS spectrum convolved with the COS model LSFs at LP3 (i.e., between the blue and red lines).

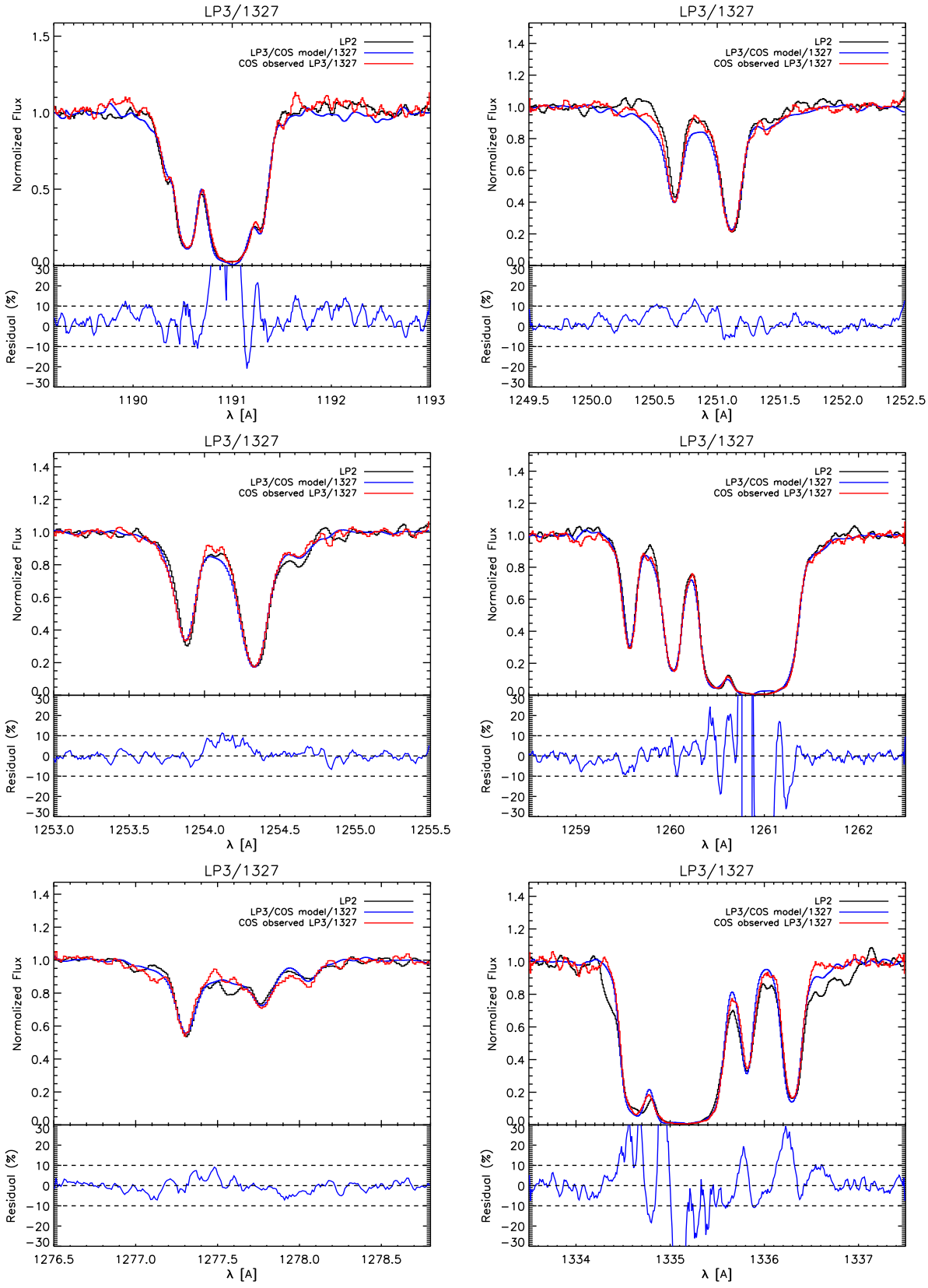
LP3/1327
LP2
LP3/COS model/1327
COS observed LP3/1327
Normalized Flux
Residual (%)
λ [A]
LP3/1327
LP2
LP3/COS model/1327
COS observed LP3/1327
Normalized Flux
Residual (%)
λ [A]
LP3/1327
LP2
LP3/COS model/1327
COS observed LP3/1327
Normalized Flux
Residual (%)
λ [A]
LP3/1327
LP2
LP3/COS model/1327
COS observed LP3/1327
Normalized Flux
Residual (%)
λ [A]
LP3/1327
LP2
LP3/COS model/1327
COS observed LP3/1327
Normalized Flux
Residual (%)
λ [A]
LP3/1327
LP2
LP3/COS model/1327
COS observed LP3/1327
Normalized Flux
Residual (%)
λ [A]

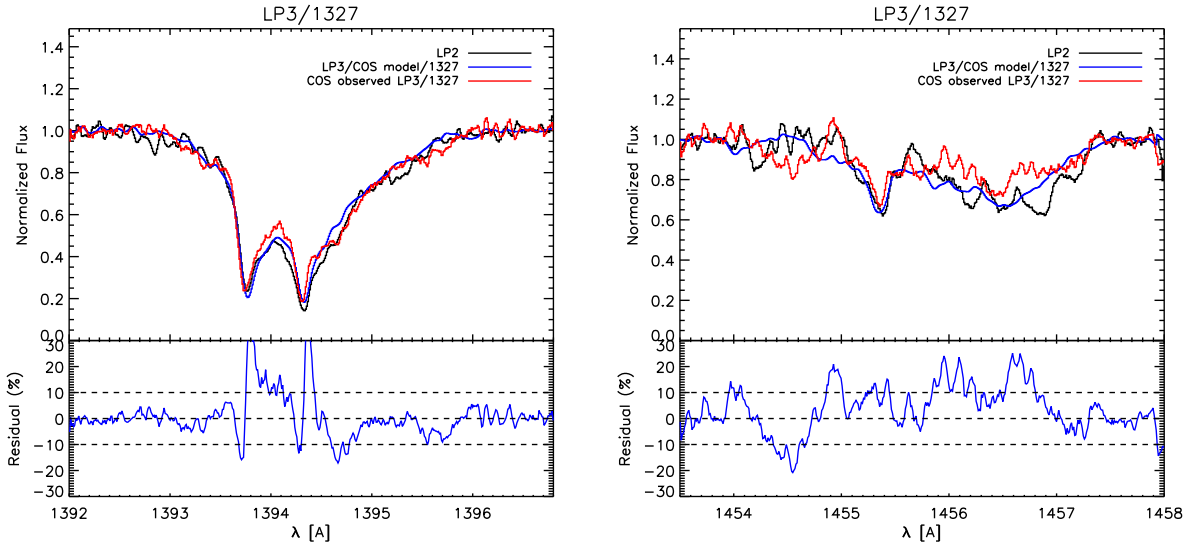

Figure 5.: Comparison between the line profiles obtained with the G130M 1327 at LP2 (black), LP3 (red), and the STIS E140M spectrum convolved with the LP3 COS model LSFs. The residuals shown in the bottom sub-panels correspond to the fractional difference between the observed COS spectra and the STIS spectrum convolved with the COS model LSFs at LP3 (i.e., between the blue and red lines).

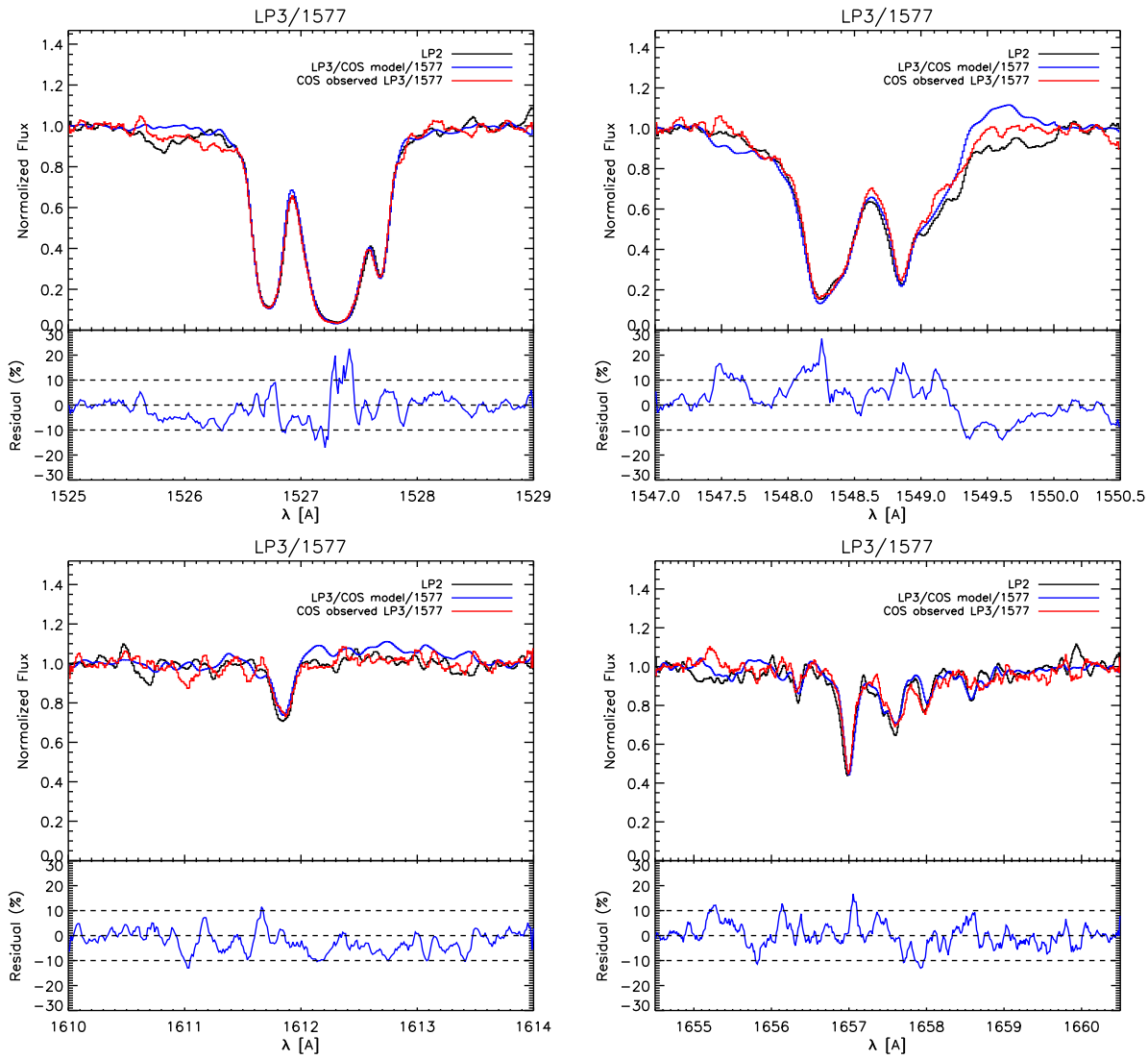

Figure 6.: Comparison between the line profiles obtained with the G160M 1577 at LP2 (black), LP3 (red), and the STIS E140M spectrum convolved with the LP3 COS model LSFs. The residuals shown in the bottom sub-panels correspond to the fractional difference between the observed COS spectra and the STIS spectrum convolved with the COS model LSFs at LP3 (i.e., between the blue and red lines).

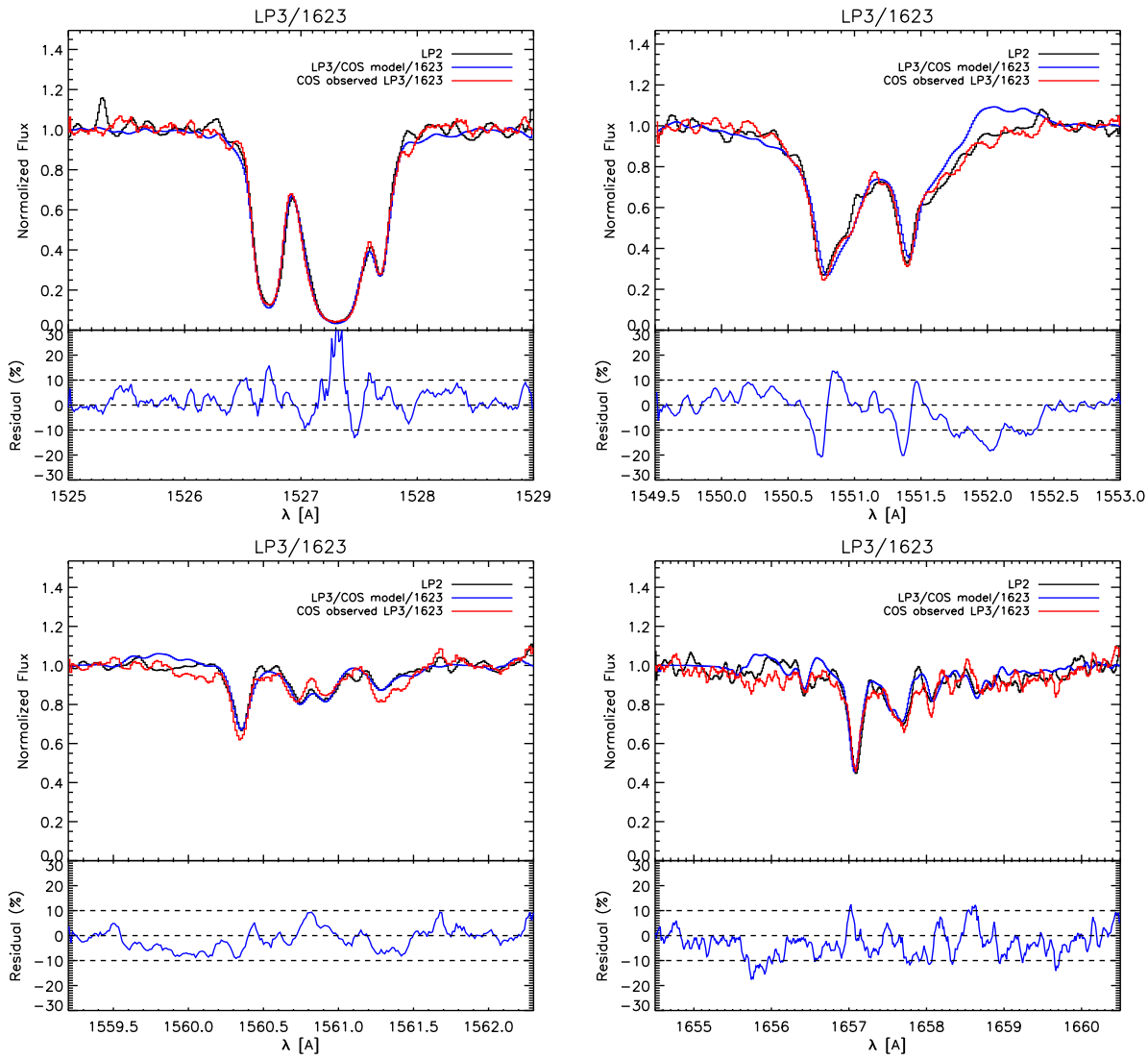

Figure 7.: Comparison between the line profiles obtained with the G160M 1623 at LP2 (black), LP3 (red), and the STIS E140M spectrum convolved with the LP3 COS model LSFs. The residuals shown in the bottom sub-panels correspond to the fractional difference between the observed COS spectra and the STIS spectrum convolved with the COS model LSFs at LP3 (i.e., between the blue and red lines).

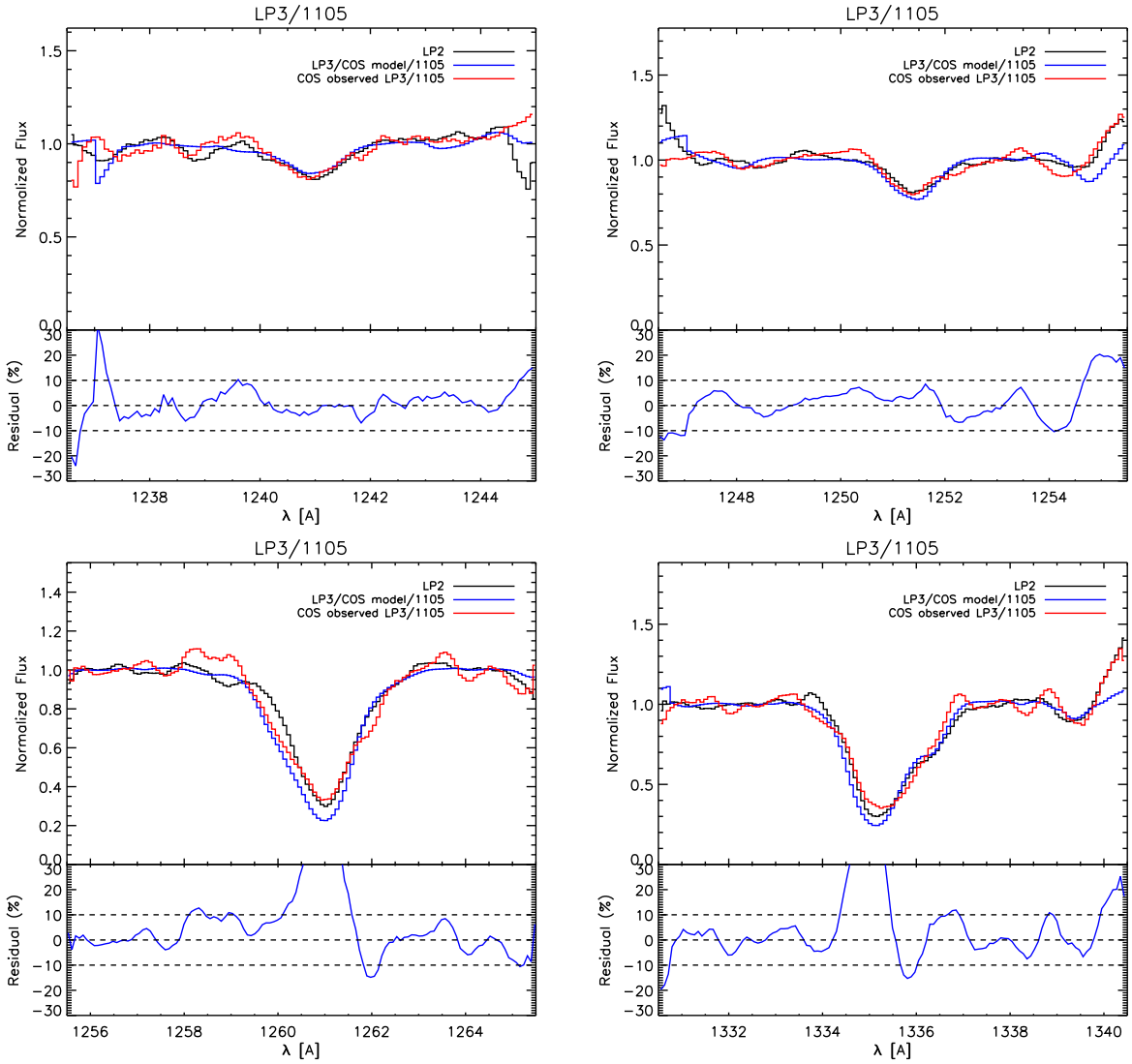
LP3/1105
LP2
LP3/COS model/1105
COS observed LP3/1105
Normalized Flux
Residual (%)
λ [A]
LP3/1105
LP2
LP3/COS model/1105
COS observed LP3/1105
Normalized Flux
Residual (%)
λ [A]
LP3/1105
LP2
LP3/COS model/1105
COS observed LP3/1105
Normalized Flux
Residual (%)
λ [A]
LP3/1105
LP2
LP3/COS model/1105
COS observed LP3/1105
Normalized Flux
Residual (%)
λ [A]

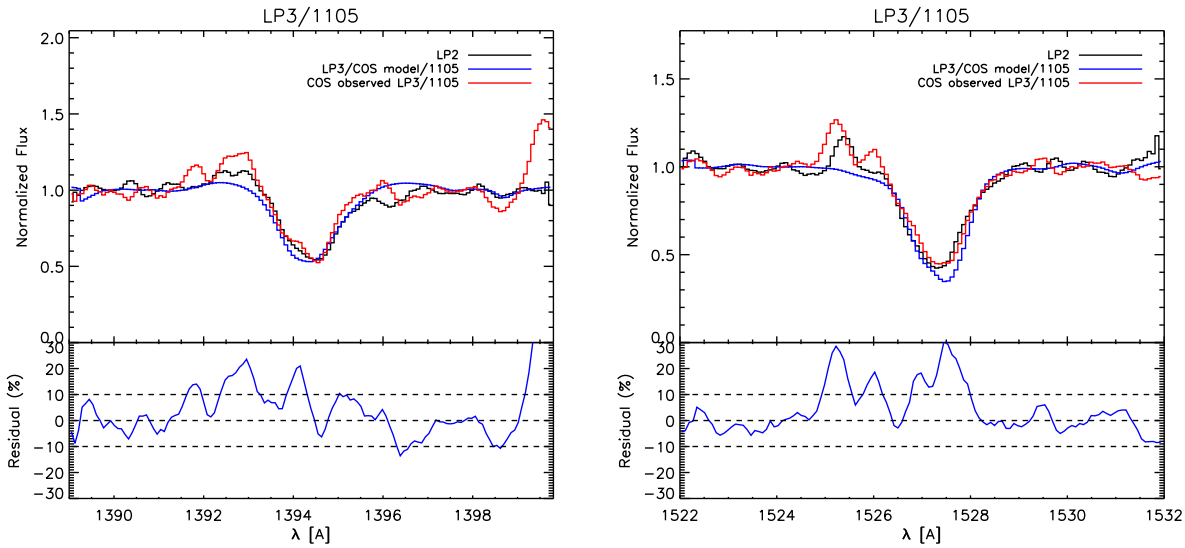

Figure 8.: Comparison between the line profiles obtained with the G140L 1105 at LP2 (black), LP3 (red), and the STIS E140M spectrum convolved with the LP3 COS model LSFs. The residuals shown in the bottom sub-panels correspond to the fractional difference between the observed COS spectra and the STIS spectrum convolved with the COS model LSFs at LP3 (i.e., between the blue and red lines).

Change History for COS ISR 2017-06

Version 1: 20 June 2017- Original Document
Version 2: 12 December 2017 - Information about G140L now included.

References

Ghavamian et al., 2009, "Preliminary Characterization of the Post-Launch Line Spread Functions of COS", COS ISR 2009-01
Sonnentrucker, P., et al., 2013, "COS FUV Dispersion Solution Verification at the New Lifetime Position". COS ISR 2013-06
Roman-Duval, J, et al., 2013, "COS/FUV Spatial and Spectral Resolution at the new Lifetime Position", COS ISR 2013-07
Roman-Duval, J., et al., 2016, "Optimization of Lifetime Position 3 of the COS/FUV Detector, COS ISR 2016-01